

Stress inhomogeneity in gap-graded cohesionless soils – a contact based perspective

D. Liu¹, C. O'Sullivan², and J.A.H. Carraro³ M. ASCE

¹PhD student, Department of Civil and Environmental Engineering, Imperial College London, London SW7 2AZ; email: d.liu18@imperial.ac.uk

²Professor of Particulate Soil Mechanics, Department of Civil and Environmental Engineering, Imperial College London, London SW7 2AZ; email: cath.osullivan@imperial.ac.uk

³ Senior Lecturer in Experimental Geotechnical Engineering, Department of Civil and Environmental Engineering, Imperial College London, London, SW7 2AZ; email: antonio.carraro@imperial.ac.uk

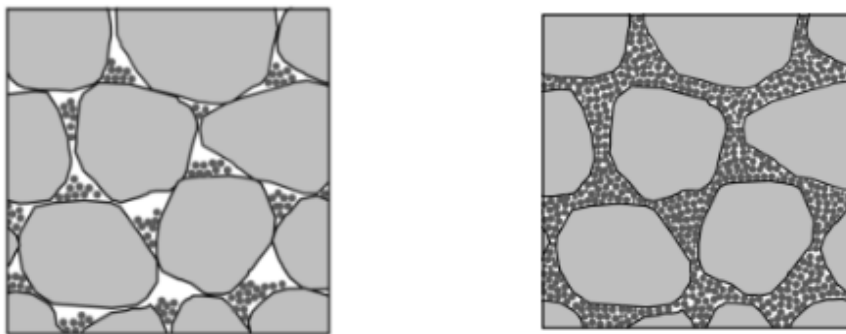
ABSTRACT:

Gap-graded cohesionless soils, comprising mixtures of fine and coarse grains, pose a particular challenge in soil mechanics. Reasoning and experimental data indicate that some of the finer grains may exist in the void space without transmitting any stress. A number of authors have proposed considering at least some of the volume of these particles along with the void space when calculating the void ratio in the case of low fines contents. The concept of a transitional fines content has been proposed, i.e. a fines content delineating materials whose behavior is dominated by the coarser grains and materials whose behavior is determined by the finer grains. This contribution uses discrete element method (DEM) simulations to explore the nature of stress transmission in gap-graded materials comprised of spherical particles. Partitioning the stress tensor by considering the contributions of the contacts between coarse particles, the contacts between coarse and fine particles, and the contacts between fine particles is shown to provide useful insight into the contribution of each type of particle to the overall stress transmission. In general, for the mixtures considered here, the coarse-coarse contacts transmit a greater range of forces and a greater average force. For the mixture with size ratio of 3.7, the range of contact force magnitudes transmitted by each contact type reduces with increasing fines content and increasing sample density. This sensitivity is more evident for the lower fines contents studied.

INTRODUCTION

A number of research studies have considered gap-graded sands comprising or binary mixtures of coarse and (non-plastic) finer sand particles. These studies have often focused on the sensitivity of the mechanical behavior to the fines content (FC), i.e. the proportion by mass of the finer sand particles in the material. For example shearing behavior was considered by Carraro et al. (2009), liquefaction by Thevanayagam et al. (2002), internal instability by Skempton & Brogan (1994) and small strain stiffness by Yang & Liu (2016). As outlined in Zuo & Baudet (2015) many of these studies have explored the idea of a threshold fines content (FC_t) that differentiates mixtures where the mechanical behavior is dominated by the finer

grains from mixtures where the coarse grains control the overall response. Considering internal erosion, Skempton & Brogan (1994) highlighted the need to consider the stress inhomogeneity in the system, specifically they considered the proportion of stress carried by the finer grains and measured it indirectly by considering the onset of seepage-induced instability in rigid-wall permeameter tests. Shire et al. (2014) and Shire et al. (2016) demonstrated that discrete element method (DEM) simulations can be used to create virtual samples of gap-graded soils in which the stress in the finer grains can be directly measured. These earlier DEM studies do not support the idea of a single FC_t value; rather they show that there is a more gradual transition, depending on the ratio of particle sizes. These DEM studies align well with ideas put forward in Skempton & Brogan (1994) who described the presence of underfilled fabrics at low fines contents and overfilled fabrics at high fines content. Referring to Figure 1 in an underfilled fabric the finer grained particles exist in the void space between the coarse particles and do not transmit stress. Where the material is overfilled the finer particles completely fill the voids between the coarse grains, so that contact between the coarse particles is inhibited and the fines themselves actively participate in stress transmission (Figure 1(b)). Skempton & Brogan did not identify a definite boundary between these fabrics associated with a single particular fines content. However Shire et al. (2014) showed that at low fines contents the material remains underfilled, irrespective of the density and at high fines contents the material remains overfilled, irrespective of density. Moreover there is an intermediate range of fines contents where the material fabric classification (overfilled or underfilled) depends on the material density (Shire et al., 2014).



(a) Underfilled fabric

(b) Overfilled fabric

Fig. 1. Illustration of underfilled and overfilled fabrics after Shire et al. (2014)

The earlier DEM studies by Shire et al. adopted a binary approach, i.e. they looked at the stress in the finer and coarse grains without considering the nature of the stress transmission between the two types of particle. They focused on average particle stresses rather than considering the distribution of stresses within each type of particle. The current study extends this earlier research by considering the contact force network rather than the particle stresses. Partition of the stress tensor to look at the contributions of the fine-fine, coarse-fine and coarse-coarse contacts separately is shown to provide useful insight into the material fabric.

NUMERICAL SIMULATION APPROACH

Following the earlier work of Shire et al. (2014) and Shire et al. (2016) the DEM simulations considered here were conducted on cubic samples, enclosed within periodic boundaries, using a modified version of the open-source molecular dynamics code Granular LAMMPS (Plimpton 1995). A simplified Hertz-Mindlin contact model was used with a particle shear modulus of 29.17 GPa and Poisson's ratio of 0.2, which proved reasonable in previous DEM studies (e.g. Huang et al. 2014). These are similar to experimentally derived values (e.g. Barreto Gonzalez 2009). In all cases the particles were initially placed randomly in diffuse (non-contacting) positions, followed by isotropic compression using a stress-controlled algorithm to achieve the initial target isotropic stress level of 500 kPa. To investigate the effect of density on the observed response, three inter-particle friction coefficients μ were used as follows: (1) $\mu = 0.001$ which generated dense samples; (2) $\mu = 0.1$, which generated medium-dense samples; (3) $\mu = 0.3$ which generated loose samples. For reasons of computational efficiency consideration was restricted to spherical particles.

A total of 11 particle size distributions were considered as illustrated in Figure 2 and four fines contents (i.e. 10%, 25%, 35%, and 50%) were used. For each fines content considered, two or three grading curves were created, each of which is identified by the size ratio, SR , which is given by $SR = \frac{D_{50}}{d_{50}}$ where D_{50} is the median diameter of the coarse grains and d_{50} is the median diameter of the finer grains. The SR values varied between 3.2 and 7.3 and correspond to two fixed ratios of maximum to minimum particle size, 5.6 and 13 respectively. Shire et al. (2016) showed that for smaller size ratios ($2 \leq SR \leq 4$) it is only at very low fines contents that the fines clearly play a reduced role in stress materials, but that at $SR=6$, the fines do not transmit stress for $FC < 25\%$.

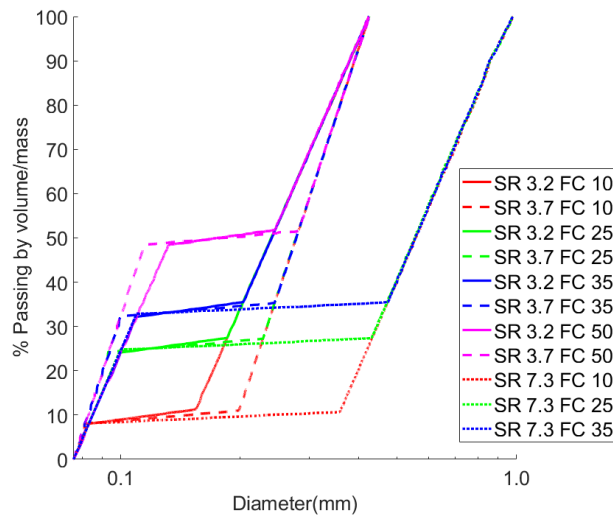


Fig. 2. Particle size distributions for the bimodal mixtures of finer and coarse particles considered here

ANALYSIS OF STRESS TRANSMISSION

Fundamentally stress is transmitted in a granular material via the contact forces. The stress tensor σ_{ij} within a volume V can be calculated as

$$\sigma_{ij} = \frac{1}{V} \sum_{C=1}^{N_c} f_i^C l_j^C \quad (1)$$

where N_c is the total number of contacts for volume V , f_i^C is the contact force vector for contact C and l_j^C is the branch vector that connects the centroids of the two particles that interact at contact C . In contrast to the earlier analyses of Shire et al. (2014) and Shire et al. (2016) who determined the stress on individual particles from the contact forces, the current study considers the distribution of the forces themselves and partitions the overall stress tensor into contributions from different contact types

Distribution of contact forces

Figure 3 presents cumulative distributions of the contact forces for three samples with $SR=3.7$. Each sample was medium dense, i.e. they were compressed with $\mu = 0.1$, and three fines contents are considered, i.e. 10%, 25%, and 50%. The sample with 10% fines is expected to be underfilled (as in Figure 1(a)), the sample with 25% fines is in the transitional zone so that the stress in the fines depends on the sample density and the sample with 50% fines is overfilled so that the fines completely fill the void space and separate the coarser grains (as in Figure 1(b)). In Figure 3 contacts between two coarse grains are identified as coarse-coarse, contacts between two fine grains are identified as fine-fine and coarse-fine relates to contacts between a fine and a coarse particle.

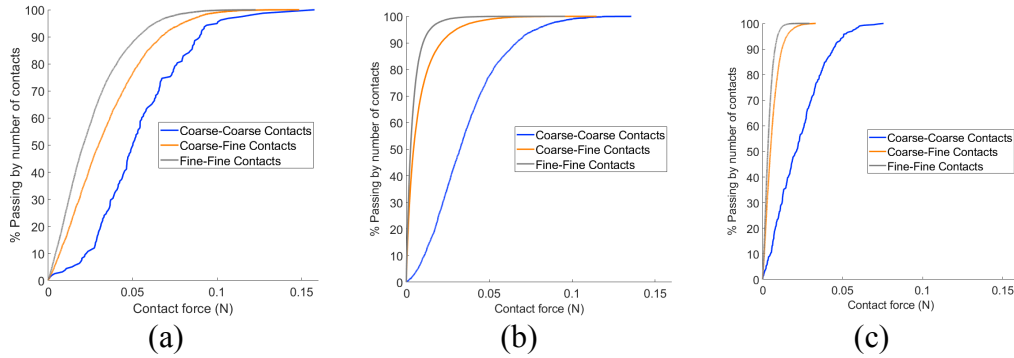


Fig. 3. Distribution of contact forces for different contact types for medium packing densities: (a) Sample SR 3.7 FC 10 (b), Sample SR 3.7 FC 25 and (c) Sample SR 3.7 FC 50

Referring to Figure 3(a) it is clear that for this underfilled material the coarse-coarse contacts transmit significantly larger forces than either the fine-fine contacts or the coarse-fine contents. The coarse-fine contacts tend to transmit forces that are intermediate in magnitude between the fine-fine and coarse-coarse contacts. The fine-fine and fine-coarse distributions are significantly smoother than the coarse-coarse contacts reflecting the relatively small proportion of coarse particles in the sample by number (approximately 20%). As the fines content increases a number of interesting observations can be made. Firstly the range of contact force magnitudes decreases for all contact types, in other words the maximum force reduces. This reduction reflects an increase in the overall number of contacts in the system. For this size ratio, the coarse-coarse contact forces are significantly larger than the fine-fine and fine-coarse contact forces for all the FC values considered.

Figure 4 also considers the distribution of contact forces in samples with $SR = 3.7$, however in this case the contact types are not differentiated and the influence of the overall packing density is considered. The reduction in the range of contact forces with increasing fines content is again evident; all the distributions are broader in Sample SR 3.7 FC 10 than they are for Sample SR 3.7 FC 50. Considering the underfilled sample (Figure 4(a), SR 3.7 FC 10), there is a clear reduction in the range of contact forces within the sample as the sample density increases. This density-dependency is more marked for the transitional sample (Figure 4(b), SR 3.7 FC 25) where the distributions of forces in the medium dense and dense samples are similar and much narrower than for the loose sample. For the overfilled sample (Figure 4(c), SR 3.7 FC 50) there is little density sensitivity.

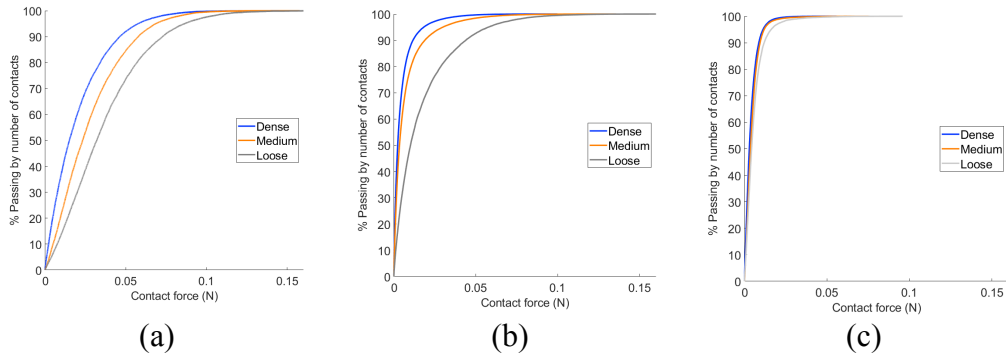


Fig. 4. Distribution of contact forces (all types combined) exploring effect of overall density for (a) Sample SR 3.7 FC 10, (b) Sample SR 3.7 FC 25 and (c) Sample SR 3.7 FC 50

Contribution of different contact types to the overall stress tensor

Thornton (2000) partitioned the stress tensor as calculated using Eq. 1 by considering the normal and tangential components of the force at each contact separately. Developing upon this idea here the overall stress tensor was decomposed into fine-fine (σ_{ij}^{ff}), fine-coarse (σ_{ij}^{fc}), and coarse-coarse (σ_{ij}^{cc}) components, where for example

$$\sigma_{ij}^{ff} = \frac{1}{V} \sum_{c=1}^{N_c^{ff}} f_i^c l_j^c \quad (2)$$

where N_c^{ff} is the total number of fine-fine contacts in volume V .

Again, considering the samples with $SR=3.7$, Figure 5 illustrates the relative contribution of each contact type to the overall stress tensor. As illustrated in Figure 5(a) the fine-fine contacts have a negligible contribution to the overall stress tensor for the underfilled sample with $FC=10\%$, irrespective of the density considered. However, for this combination of SR and FC values while the vast majority of the stress is transmitted via the coarse-coarse contacts, the fine-coarse contacts have a finite contribution. This must reflect the presence of individual fine particles trapped between two coarse grains. As the fines content increases to 25% (Figure 5(b)), the dominance of the coarse-coarse contacts reduces so that for the densest sample they transmit less than 50% of the overall stress. For this value of SR , in the densest packing the coarse-fine contacts make the greatest contribution to the

overall stress tensor; the contribution of the coarse-coarse contacts increases as the packing density reduces. For the overfilled material with FC=50%, the coarse-fine contacts make the greatest contribution to the overall stress at all densities considered. The coarse-coarse contacts make the smallest contribution to the overall stress for all densities. Interestingly, the distribution of stress between the fine-fine and coarse-fine contacts is density-dependent for this high fines content. Partitioning the stress tensor in this way clearly shows that when FC=50% the fine particles are indeed separating the coarse grains, preventing significant stress transmission via coarse-coarse contacts as schematically illustrated in Figure 1(b).

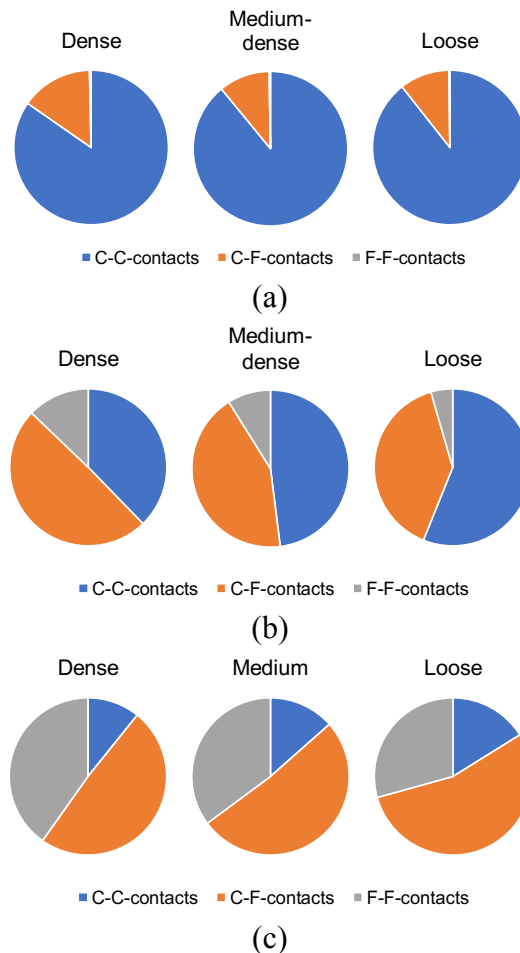


Fig. 5. Partition of stress tensor by contact type exploring the effect of overall density – segment size illustrates the proportion of stress transmitted by each contact type: (a) Sample SR 3.7 FC 10, (b) Sample SR 3.7 FC 25 and (c) Sample SR 3.7 FC 50

As noted above, Shire et al. (2016) highlighted the need to consider both size ratio and fines content. Figure 6(a) considers three medium-dense samples with SR=3.7 and three medium-dense samples with SR=7.3. It is clear from Figure 6(a) that as the size ratio increases, the coarse-coarse contact contribution becomes more dominant while the fine-fine contact contribution diminishes. For example, for FC=10% the trapping of individual fine particles between two coarse particles is less evident at SR=7.3 than it is at SR=3.2, as reflected in the almost negligible contribution of the fine-coarse contacts to the overall stress when SR=7.3. Note that for these size ratios the coarse-coarse contacts make a significant contribution to the overall stress transmission even at FC=35%, indicating that the material

cannot be considered completely fines-dominated at FC=35%. This size ratio dependency is summarized in Figure 6(b), where it is clear that the stress transmitted by the fines reduces with increasing size ratio for the FC values considered here.

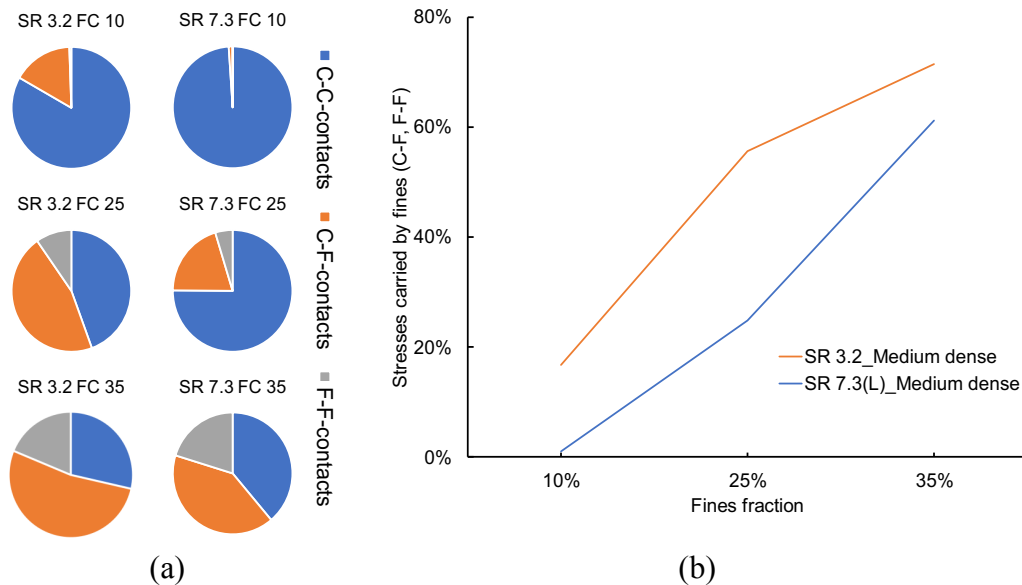


Fig. 6. Partition of stress tensor by contact type exploring effect of size ratio by comparing medium dense samples with SR=3.2 and SR=7.3:

(a) Pie chart illustration of contribution of contact types to overall stress tensor (segment size illustrates the proportion of stress transmitted by each contact type); (b) Variation in contribution to stress by contacts involving fine particles with fines fraction

CONCLUSIONS

Understanding the nature of stress transmission in gap-graded materials is important to inform decisions about how to interpret the mechanical behavior of these materials. Recent research studies into liquefaction, small strain stiffness, and internal instability have all highlighted the need to consider these types of granular materials in a fundamental way. Shire et al. (2014) and Shire et al. (2016) demonstrated that DEM simulations can advance understanding, however this earlier research considered particle stresses, rather than looking at the more fundamental forces between the particles. The current study has used DEM and broadly followed the approach of Shire et al., however it has considered both the distribution of contact forces and the contribution to the overall stress of different classes (types) of contact.

The following main points can be made:

1. There is a difference in the distribution of contact force magnitudes when the fine-fine, coarse-coarse and coarse-fine contacts are considered separately. For the mixtures considered here the coarse-coarse contacts transmit a greater range of forces and a greater average force.
2. For the sample with SR=3.7 considered in detail here the range of contact force magnitudes transmitted by each contact type reduces with increasing fines content. This can be linked to the increase in coordination number (i.e. the number of contacts in the sample).

3. Again considering the sample with $SR=3.7$, the range of contact forces within the material reduces with increasing sample density and this sensitivity is more evident for the lower fines contents.
4. Partitioning the stress tensor by contact type provides useful insight into the stress transmission and role of the different particle types in stress transmission.

ACKNOWLEDGEMENTS

Mr. Deyun Liu is supported by the Chinese Scholarship Council, and an Imperial College London Dixon Scholarship. The high performance computing resources at Imperial College London were used to run the DEM simulations.

REFERENCES

- Barreto Gonzalez, D., 2009. *Numerical and experimental investigation into the behaviour of granular materials under generalised stress states*. University of London.
- Carraro, J.A.H., Prezzi, M. & Salgado, R., 2009. Shear Strength and Stiffness of Sands Containing Plastic or Nonplastic Fines. *Journal of Geotechnical and Geoenvironmental Engineering*, 135(9), pp.1167–1178.
- Huang, X. et al., 2014. Exploring the influence of interparticle friction on critical state behaviour using DEM. *International Journal for Numerical and Analytical Methods in Geomechanics*, 38(12).
- Plimpton, S., 1995. Fast Parallel Algorithms for Short-Range Molecular Dynamics. *Journal of Computational Physics*, 117(1), pp.1–19.
- Shire, T. et al., 2014. Fabric and Effective Stress Distribution in Internally Unstable Soils. *Journal of Geotechnical and Geoenvironmental Engineering*, 140(12), pp.1–11.
- Shire, T., O’Sullivan, C. & Hanley, K.J., 2016. The influence of fines content and size-ratio on the micro-scale properties of dense bimodal materials. *Granular Matter*, 18(3).
- Skempton, A.W. & Brogan, J.M., 1994. Experiments on piping in sandy gravels. *Géotechnique*, 44(3), pp.565–567.
- Thevanayagam, S. et al., 2002. Undrained Fragility of Clean Sands, Silty Sands, and Sandy Silts. *Journal of Geotechnical and Geoenvironmental Engineering*, 128(10), pp.849–859. Available at: [http://www.scopus.com/inward/record.url?eid=2-s2.0-0036799511&partnerID=tZOtx3y1%5Chttp://ascelibrary.org/doi/10.1061/\(ASCE\)1090-0241\(2002\)128:10\(849\)](http://www.scopus.com/inward/record.url?eid=2-s2.0-0036799511&partnerID=tZOtx3y1%5Chttp://ascelibrary.org/doi/10.1061/(ASCE)1090-0241(2002)128:10(849)).
- Thornton, C., 2000. Numerical simulations of deviatoric shear deformation of granular media. *Géotechnique*, 50(1), pp.43–53. Available at: <http://www.icevirtuallibrary.com/content/article/10.1680/geot.2000.50.1.43>.
- Yang, J. & Liu, X., 2016. Shear wave velocity and stiffness of sand: the role of non-plastic fines. *Geotechnique*, 66(6), pp.500–514.
- Zuo, L. & Baudet, B.A., 2015. Determination of the transitional fines content of sand-non plastic fines mixtures. *Soils and Foundations*, 55(1), pp.213–219. Available at: <http://dx.doi.org/10.1016/j.sandf.2014.12.017>.